Supplementary

Facile etching process for porous structure of hexagonal boron nitride as a catalyst support by metal oxides in low-temperature

Myeung-Jin Lee[1,†], Donghyeok Kim[1,†], Nahea Kim[1], Sang-Hyeok Seo[1], Dahye Park[1], Tae-hyung Kim[2], Bora Jeong[1], and Hong-Dae Kim[1,*]

† These authors contributed equally to this work.

[1] Ulsan Technology Application Division, Korea Institute of Industrial Technology, Ulsan 44413, Republic of Korea

[2] Korea Institute of Limestone and Advanced Materials, Danyang-gun 27003, Republic of Korea

* Hong-Dae Kim. Tel.: +82)52-980-6650, E-mail address: hdkim@kitech.re.kr

Academic Editor: Firstname Lastname

Received: date
Revised: date
Accepted: date
Published: date

Copyright: © 2026 by the authors. Submitted for possible open access publication under the terms and conditions of the Creative Commons Attribution (CC BY) license.

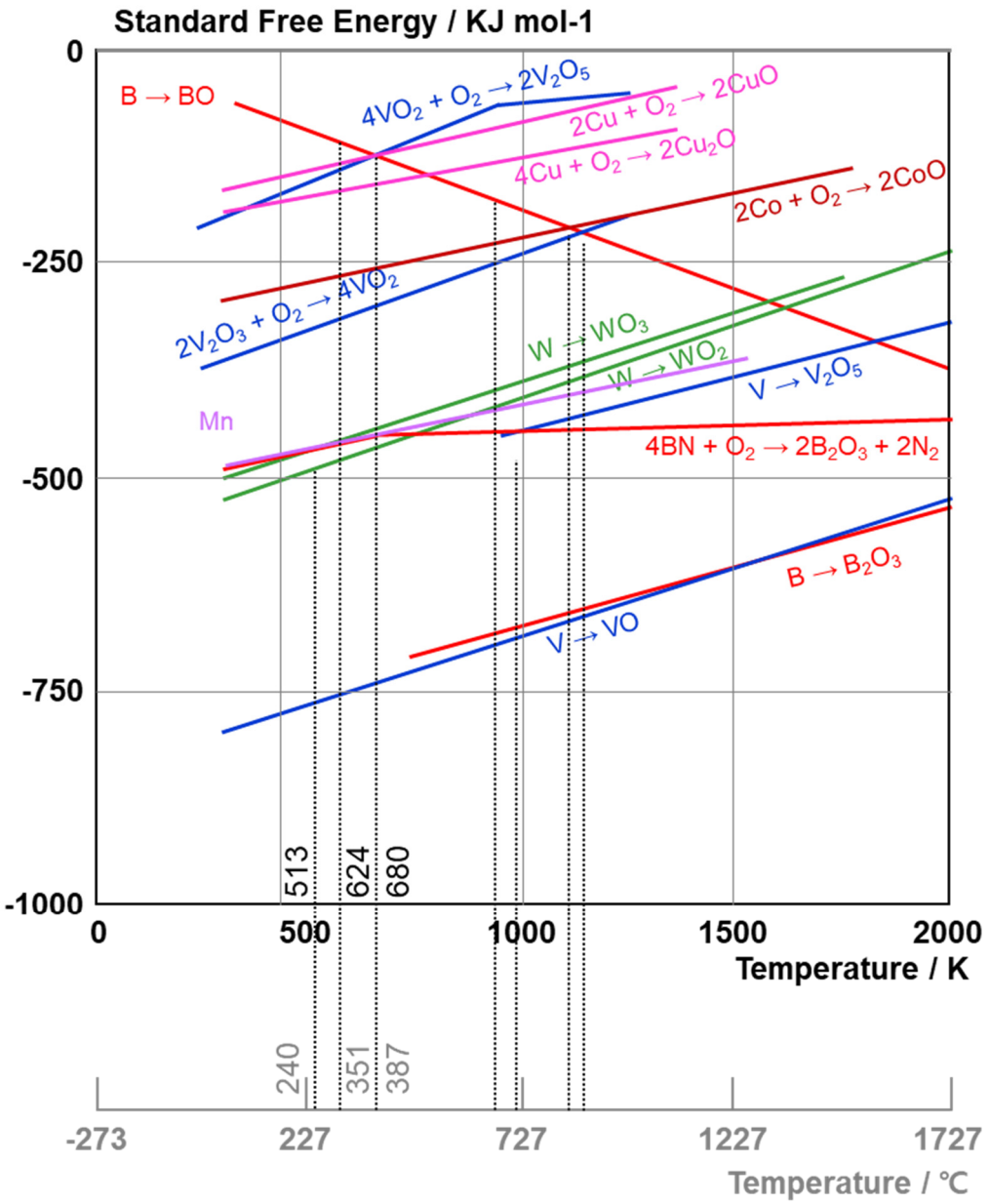


Figure S1. Ellingham diagram for oxidation reactions of boron nitride (BN) and several metal cation

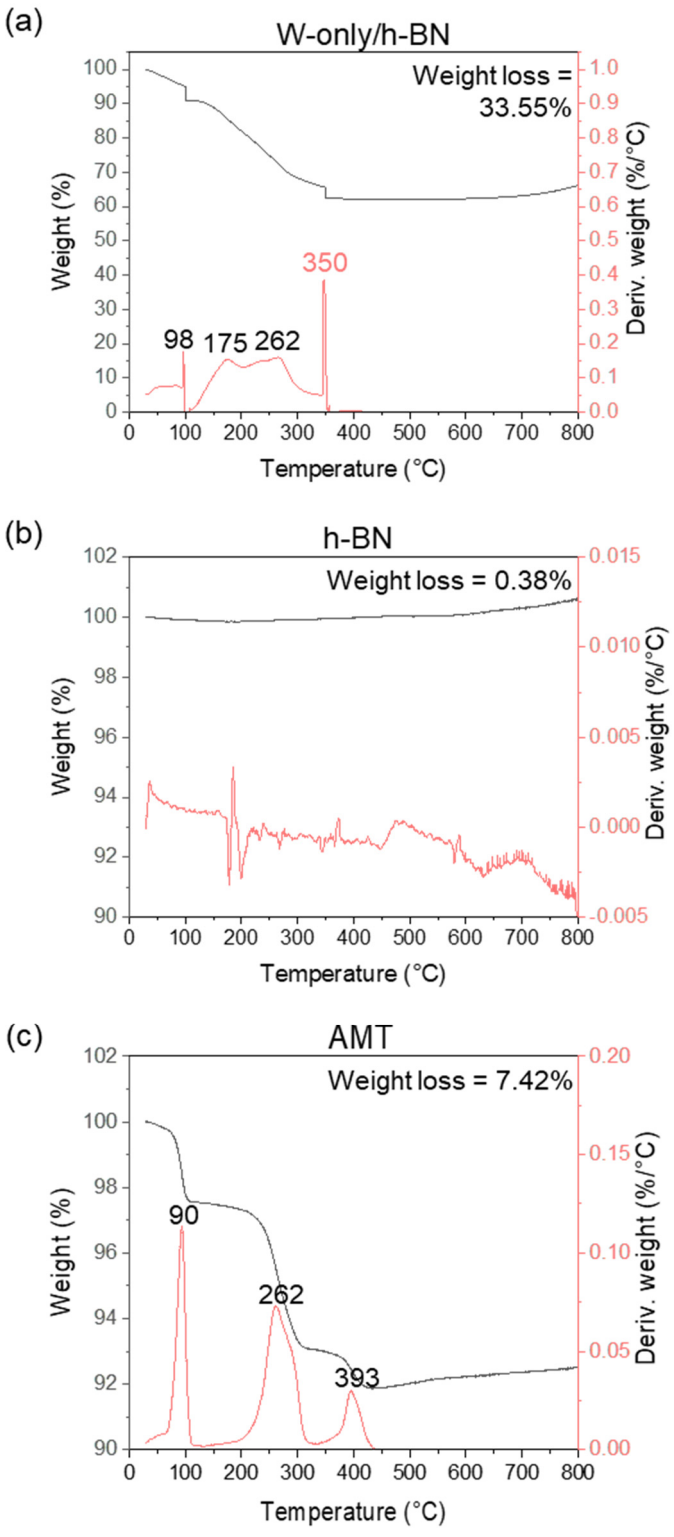


Figure S2. TGA results for (a) W-only/h-BN, (b) pristine h-BN, and (c) precursors of tungsten (AMT)

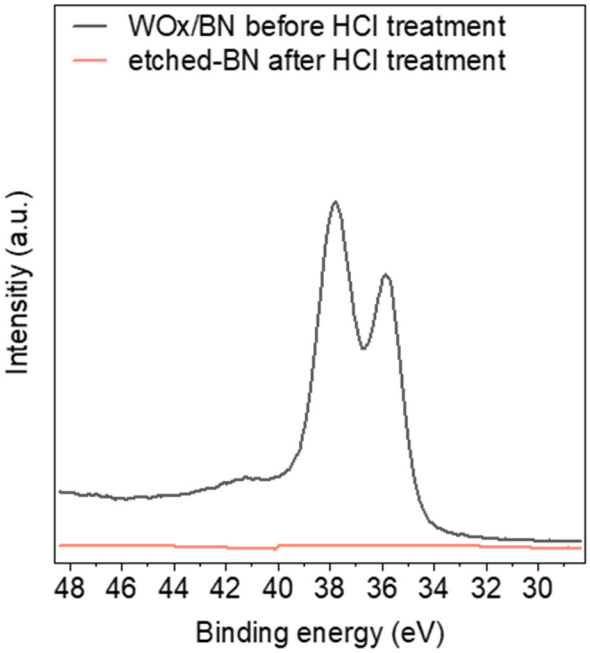


Figure S3. W 4f spectra of X-ray photoelectron spectroscopy to observe the removal of WOx (metal oxides) through HCl treatment

Table S1. Textural properties. Specific surface area (S_{BET}), pore diameter (D_P), and pore volume (V_P) for pristine h-BN and etched h-BN by the several metal cation

	S_{BET}	D_p	V_p
Pristine h-BN	14.07	12.12	0.05
Etched-BN by Co	29.05	13.84	0.11
Etched-BN by Mn	26.18	12.87	0.08
Etched-BN by Ce	30.22	11.23	0.09
Etched-BN by V	33.80	19.63	0.18
Etched-BN by W	39.83	21.79	0.21
Etched-BN by Cu	24.33	12.94	0.16
Etched-BN by Ni	28.18	16.33	0.17

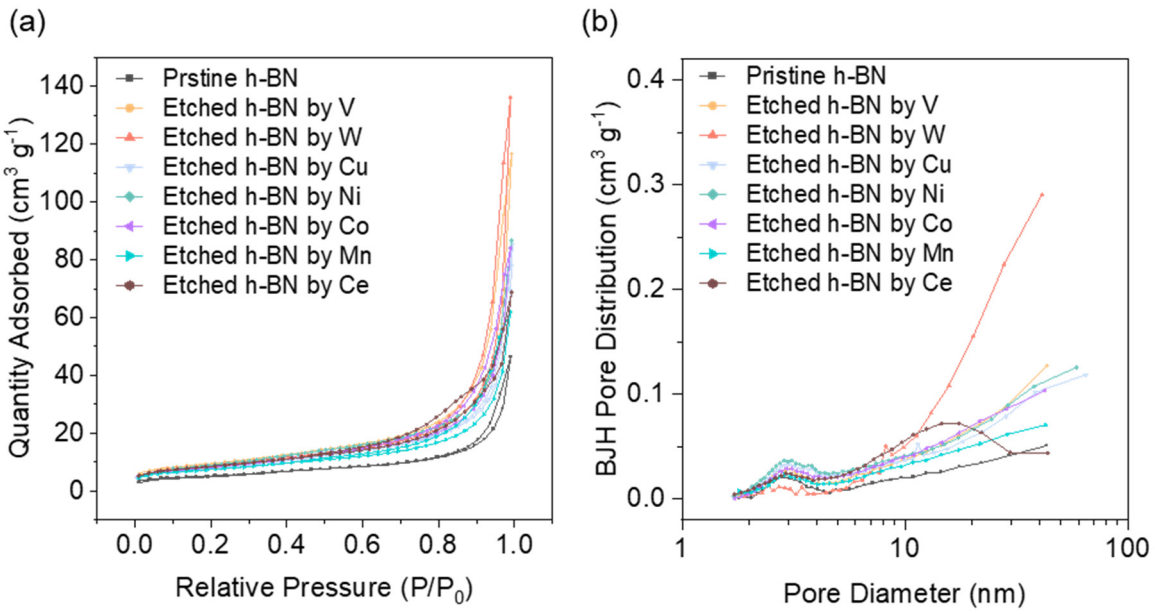


Figure S4. (a) BET hysteresis curves based on N_2–adsorption–desorption and (b) BJH pore distributions for pristine h-BN and etched h-BN by the several metal cation

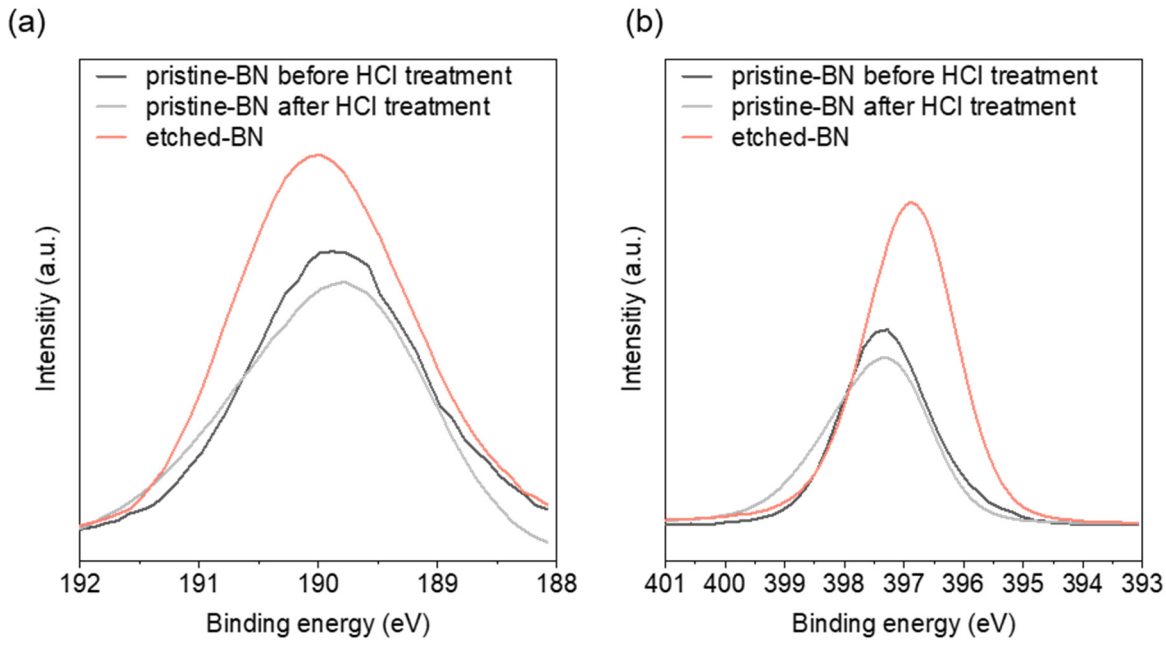


Figure S5. (a) B 1s and (b) N 1s spectra of X-ray photoelectron spectroscopy

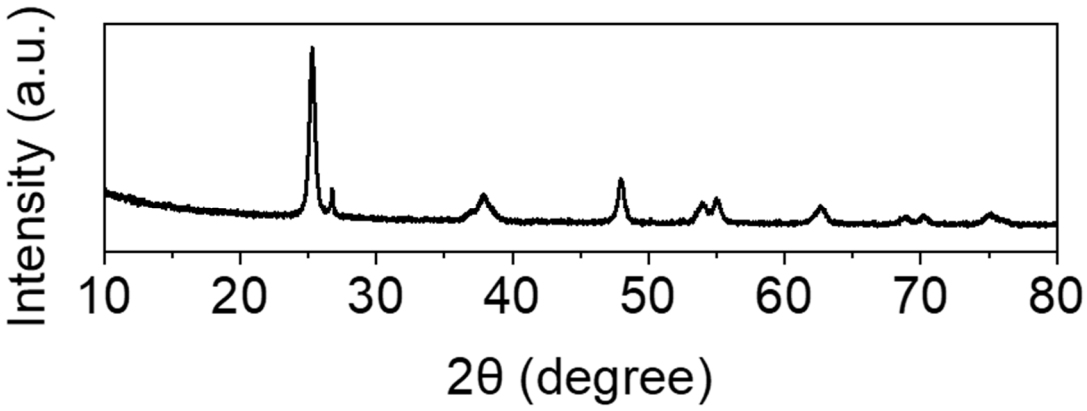


Figure S6. X-ray diffraction patterns of CuNi/TiO_2 with etched h-BN catalyst

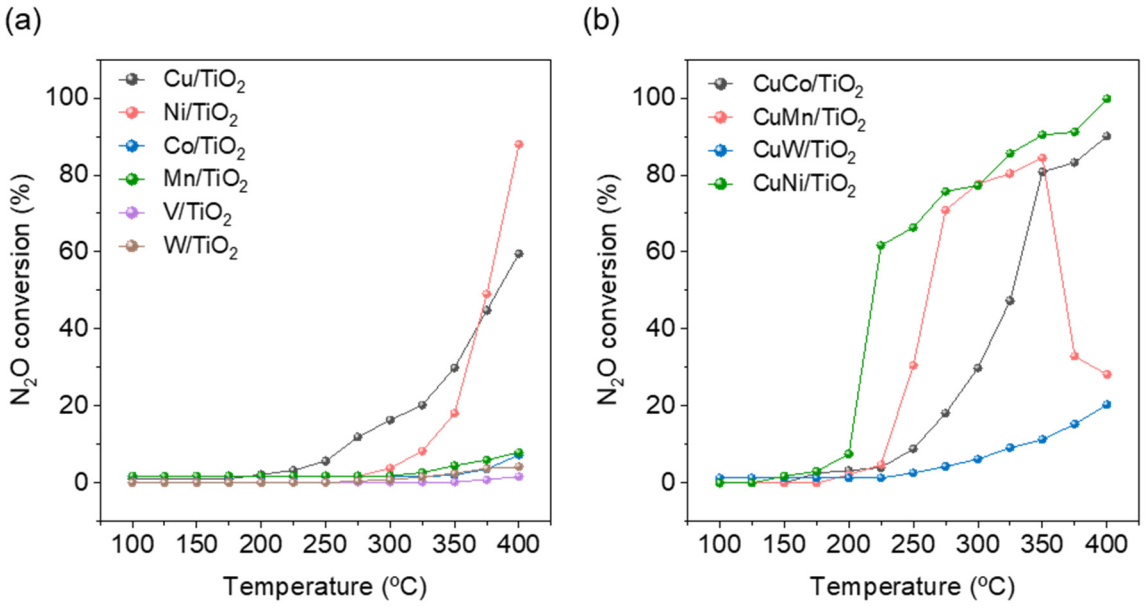


Figure S7. N_2O conversion for (a) one-component and (b) two-components catalyst under gas conditions of [N_2O] = 180 ppm, [CO] = 540 ppm, [N_2] = balance, and GHSV = 60,000 h^{-1} over the temperature range of 100–400 °C.

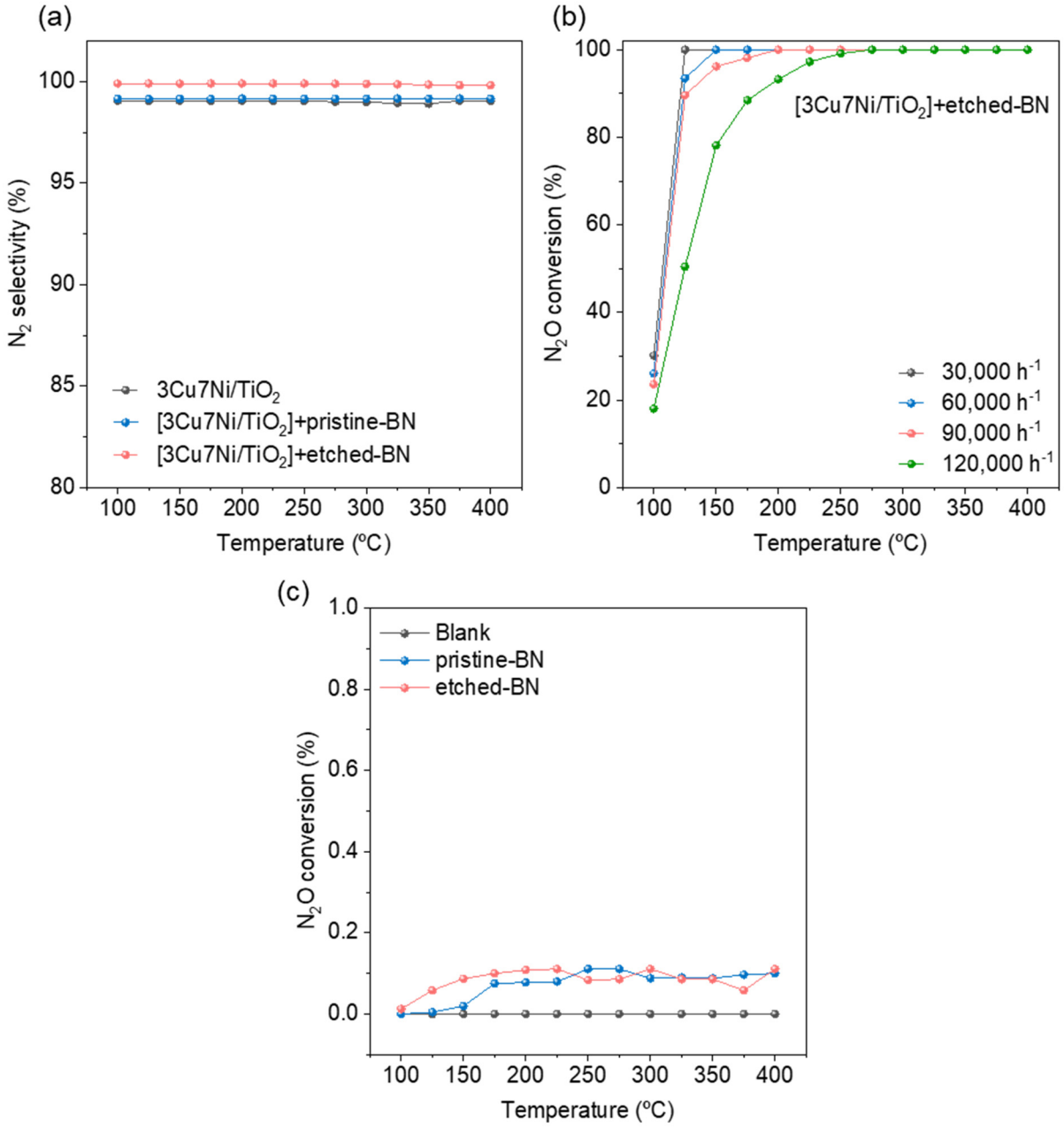


Figure S8. (a) N_2 selectivity and N_2O conversion by (b) various GHSV and (c) blank test with only h-BN

Table S2. Textural properties for 3Cu7Ni/TiO_2 with/without pristine h-BN and etched h-BN

	S_{BET}	D_p	V_p
[3Cu7Ni/TiO_2]	71.86	0.29	16.63
[3Cu7Ni/TiO_2]+pristine h-BN	63.78	0.24	15.59
[3Cu7Ni/TiO_2]+etch h-BN	78.19	0.31	16.56

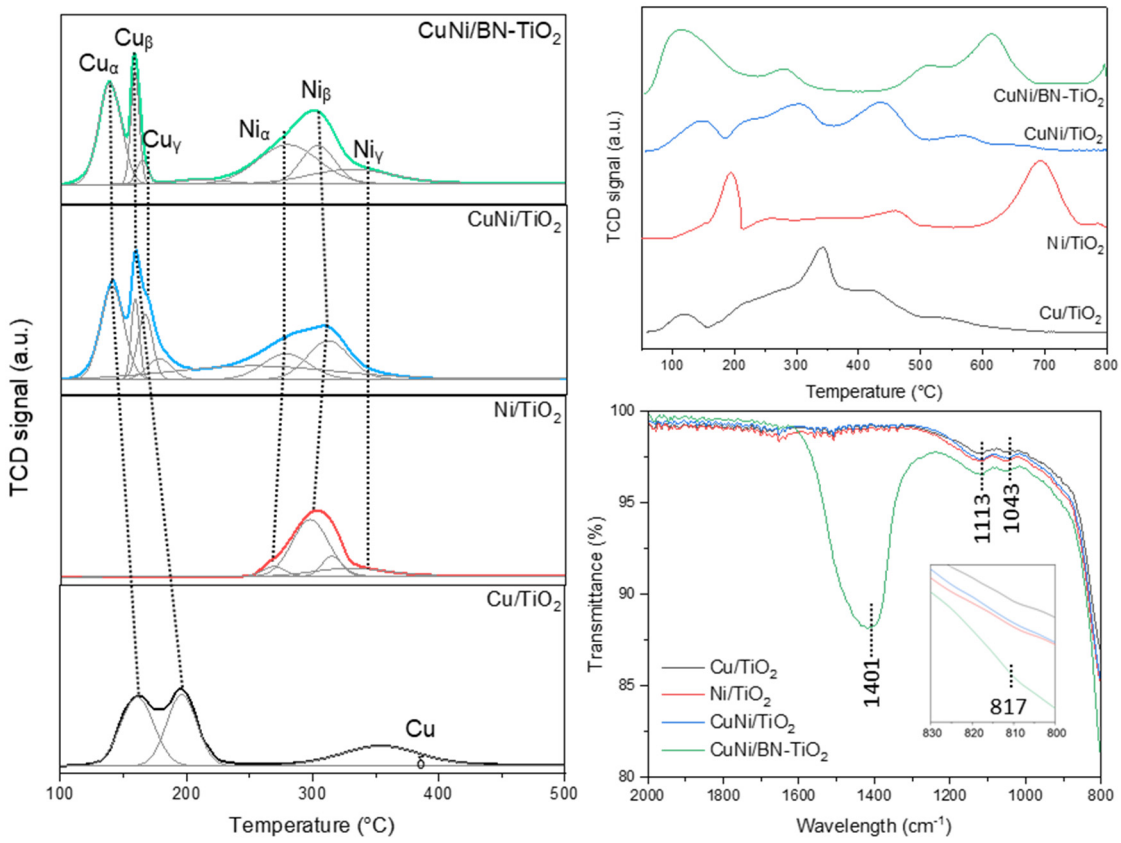


Figure S9. (a) Hydrogen-temperature-programmed-reduction (H_2-TPR) profiles, (b) CO-temperature-programmed-desorption (CO-TPD) profiles, and (c) investigated FT-IR spectra for Cu-only/TiO_2, Ni-only/TiO_2, CuNi/TiO_2, and CuNi/BN-TiO_2.

Table S3. Calculated amounts of H_2-consumption for Cu-only/TiO_2, Ni-only/TiO_2, Cu-Ni/TiO_2, and Cu-Ni/BN-TiO_2.

	H_2-consumption							
Catalyst	Cu_α	Cu_β	Cu_γ	Cu_δ	Ni_α	Ni_β	Ni_γ	Total
Cu-only/TiO_2	0.43	0.48	-	0.6	-	-	-	1.51
Ni-only/TiO_2	-	-	-	-	0.25	0.63	0.19	1.07
Cu-Ni/TiO_2	0.61	0.25	0.37	-	0.46	0.62	0.24	2.55
Cu-Ni/BN-TiO_2	0.84	0.25	0.17	-	0.63	0.34	0.32	2.55

Table S4. Calculated amounts of CO-consumption for Cu-only/TiO_2, Ni-only/TiO_2, Cu-Ni/TiO_2, and Cu-Ni/BN-TiO_2.

	CO-desorption		
Catalyst	Low	High	Total
Cu-only/TiO_2	0.61	0.08	0.69
Ni-only/TiO_2	0.42	0.49	0.91
Cu-Ni/TiO_2	0.58	0.09	0.67
Cu-Ni/BN-TiO_2	0.38	0.51	0.89